JEH1104(070)

Journal of Enhanced Heat Transfer, 11(4) 451–457 (2004)
Reprints available directly from the publisher.
Photocopying permitted by license only.

Numerical Verification of the Field Synergy Principle for Turbulent Flow

ZENG MIN & TAO WEN-QUAN

State Key Laboratory of Multiphase Flow in Power Engineering,
School of Energy and Power Engineering Xi'an Jiaotong University,
Shaanxi, Xi'an 710049, China

In this paper, the field synergy principle is validated numerically by two turbulent flow and heat transfer examples. The results show that the field synergy principle can also be applied to turbulent flow situations.

Key words: field synergy principle, turbulent flow, numerical simulation

* Corresponding author: wqtao@mail.xjtu.edu.cn

This article appears in the Proceedings of the 3rd International Symposium on Heat Transfer and Energy Conservation (Guangzhou, China, Jan. 11–14, 2004). Editing was conducted to make the paper suitable for *Journal of Enhanced Heat Transfer.*

NOMENCLATURE

A	surface area, m^2	k	turbulent kinetic energy, m^2/s^2
C_p	specific heat capacity, J/(kg · K)	L	length, mm
d	plate thickness, mm	Nu	Nusselt number
H	duct height or transverse distance plates (mm)	Pr	Prandtl number
$\vec{U}$	velocity vector	Q	total heat in a cycle, W
u, v	velocity component in x and y direction, m/s	Re	Reynolds number
x, y	Cartesian coordinates intersection angle between velocity and temperature gradient fluid density, Kg/m^3, turbulent energy dissipation, m^2/s^3	T	temperature, °C
		Subscripts	
Int	integral, $\iint_\Omega \rho C_p(\vec{U} \cdot gradT)dA$, W	in	inlet
		w	wall

INTRODUCTION

Guo et al. (1998) and his co-workers (Wang et al., 1998) proposed a novel concept for enhancing convective heat transfer of parabolic flow: the reduction of the intersection angle between velocity and temperature gradient can effectively enhance convective transfer. Tao et al. (2002) extended the major idea of this novel concept to the elliptic convective heat transfer situation. This novel concept will be referred to as the *field synergy principle* (FSP) hereafter.

The major idea of the FSP is briefly reviewed here. By integrating the energy equation over the entire domain, we obtain following expression of the convective term

$$\iint_\Omega \rho C_p \left(\vec{U} \cdot gradT\right) dxdy = \iint_\Omega (\rho C_p \left|\vec{U}\right| \left|gradT\right| \cos\theta) dxdy \qquad (1)$$

It actually represents the energy transferred by convection. Thus it is clear that for a given flow rate and temperature difference, a better synergy (i.e., decreasing the intersection angle θ between the velocity vector and the temperature gradient) will make the integration $\iint_\Omega \rho c_p \left(\vec{U} \bullet gradT\right) dxdy$ larger—i.e., enhancing the heat transfer.

The above idea has been widely validated for many laminar convective heat transfer problems. The purpose of this paper is to show by numerical examples that the above idea is also valid for turbulent flow situations. The turbulent flow and heat transfer across discrete parallel and staggered plates will be carefully examined by adopting a low Reynolds number turbulence model. At first, we check that whether the variation trend of the above integration with the Reynolds number is the same as the variation of the averaged Nusselt number, which is computed from the overall heat transfer rate of the entire domain. Then, under the same mass flow rate, we change the thickness of the plate to see if the intersection angle variation is consistent with the variation of the heat transfer rate. In addition, we compare the heat transfer characteristics of parallel and staggered plate arrays. Finally, some remarks are concluded.

PHYSICAL PROBLEMS

The parallel and staggered plate arrays considered for the numerical simulation are shown in Figure 1 and Figure 2, respectively. The computation condition is as follows: $L1 = L2$, $H/L1 = 1$, $d/L1 = 0.2 \sim 0.4$. Air is used as the heat transfer medium. The computation domain is surrounded by the broken lines. All the flows computed are assumed to be turbulent, and the

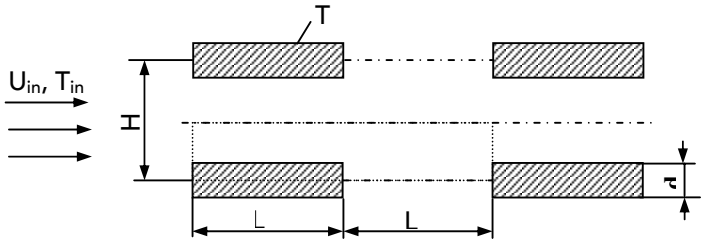

FIGURE 1. Flow and heat transfer across discrete parallel plates.

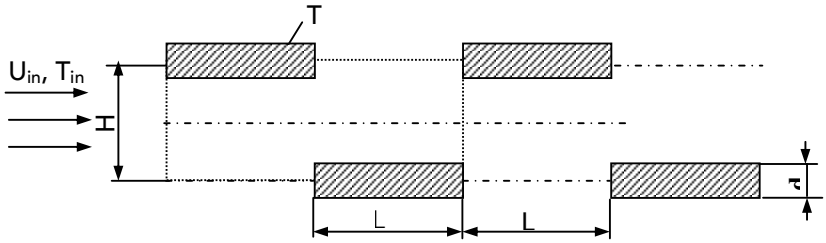

FIGURE 2. Flow and heat transfer across discrete staggered plates.

low Reynolds number k–ε model of Jones/Lauder (Jones and Lauder, 1973) is adopted. For the validation of FSP, numerical computations are carried out to obtain the integral of $\iint_{\Omega} \rho C_p \left(\vec{U} \bullet grad T\right) dA$ over the whole computation domain and the averaged Nusselt number for the configuration studied. For the simplicity of presentation, the integral will be represented by "*Int*" hereafter.

NUMERICAL METHOD

The numerical modeling approach is now briefly described. The governing equations are omitted here to save space. They are discretized by the finite volume method on a staggered grid system (Tao, 2000; Tao, 2001). The power-law scheme is used to discretize the convection and diffusion terms. The velocity/pressure coupling is achieved through the use of the continuity equation by applying the SIMPLEC algorithm (Van Doormaal and Raithby, 1984). The resulting algebraic equations are solved by using the ADI-TDMA.

The velocity boundary conditions at the wall are of the no-slip type ($u = v = k = \varepsilon = 0$). The surface temperature is kept constant.

Periodicity conditions are used at the inlet and outlet of the flow domain in order to represent a fully developed flow field for the enhanced passage calculated. Fully developed flow requires identical inlet and outlet profiles for the velocities, turbulent kinetic energy, and turbulent energy dissipation. The driving force for the flow is a constant pressure difference that exists between the inlet and outlet of the passage. It should be noted that for the periodic condition of the temperature, it is the dimensionless temperature that must be identical between the inlet and outlet.

To implement the low-Re k–ε model, a very fine grid mesh is used adjacent to the plate surface. The mesh size is then gradually expanded away from the surface, as shown in Figure 3. The first near-wall grid point is located well within the laminar sublayer ($y^+ = 0.1$) for all computations. The number of grids outside the laminar sublayer is always larger than 85. Grid independency tests are performed for the two examples. Figure 4 shows the grid independency test results of the first case. In the figure, Q represents the cyclic heat

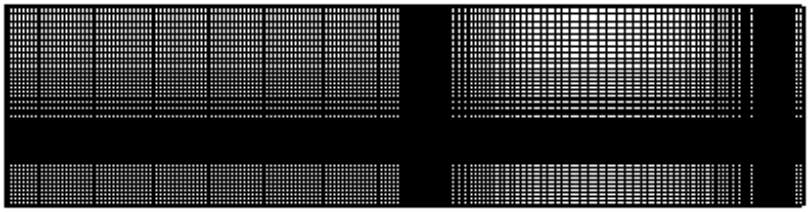

FIGURE 3. Schematic grid distribution of the first case.

transfer rate. The grid system of 304 × 92 is adopted for all computations. The convergence criterion for the iteration is that the normalized mass residual (the maximum residual of control-volume divided by the total mass flow rate) is less than 1×10^{-6}.

RESULTS AND DISCUSSION

Heat Transfer for Fluid Flowing Across Discrete Parallel Plates

For comparison purposes, the parameters $L1$, $L2$, and H are kept constant with the thickness of d varying from 2 mm to 4 mm. The characteristic length of the Nusselt number and Reynolds number is taken as $2H$ for all cases. In the computation of parallel plates the Reynolds number varies from 5,000 to 15,000.

The numerical results are shown in Figures 5, 6 and 7. Two features may be noted. First, the variation trends of *Int* and *Nu* with *Re* are very similar, and both *Int* and *Nu* become higher with the increase in thickness d. Second, the intersection angle θ between the velocity vector and the temperature gradient decreases with the increase of plate thickness d at the same mass flow. The same features can be observed from the results for the staggered plate array. These results are consistent with the major idea of FSP, thus proving that the field synergy principle can also be applied to the turbulent flow.

[AU: THERE ARE STRANGE SYMBOLS IN THE LABELS HERE AND ELSEWHERE; THESE WERE IN THE ORIGINALS TOO, SO I COULDN'T CHANGE THEM. PLEASE ADVISE]

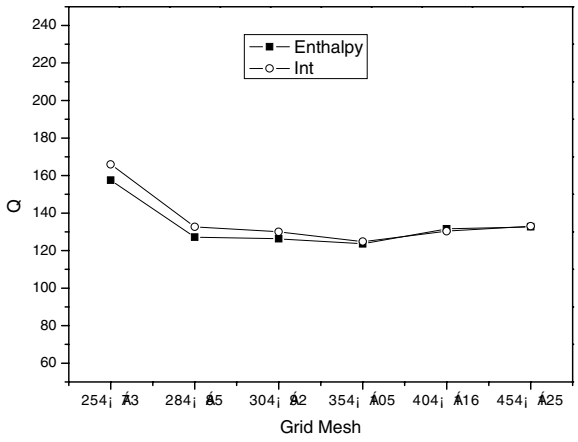

FIGURE 4. Grid independency test of the first case.

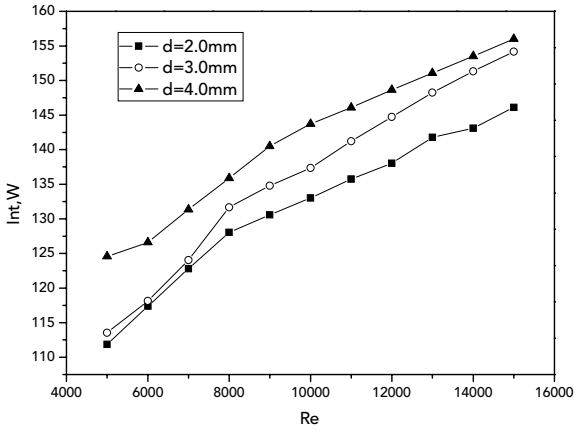

FIGURE 5. The variation of *Int* with Reynolds number (flow across discrete parallel plates).

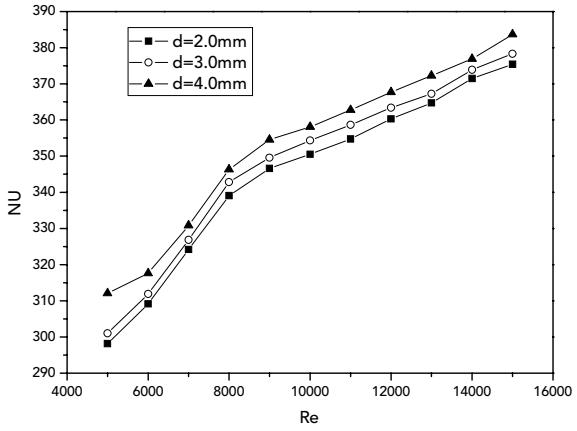

FIGURE 6. The variation of *Nu* with Reynolds number (flow across discrete parallel plates).

From Figure 7 it can be seen that for a fixed plate thickness d, the intersection angle θ increases with the mass flow rate, indicating some deterioration of the synergy between velocity and temperature gradient. Although the overall convective heat transfer increases with the Reynolds number (Figs. 5 and 6), the increasing tendency gradually becomes less and less. This feature is common to all convective heat transfer problems, leading to the general expression of $Nu \sim Re^n$ with n less than 1.

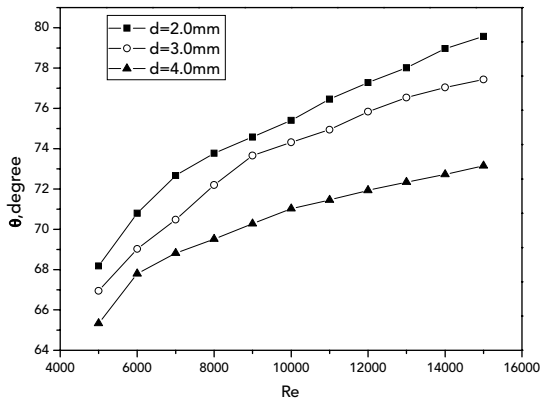

FIGURE 7. The variation of θ with Reynolds number (flow across discrete parallel plates).

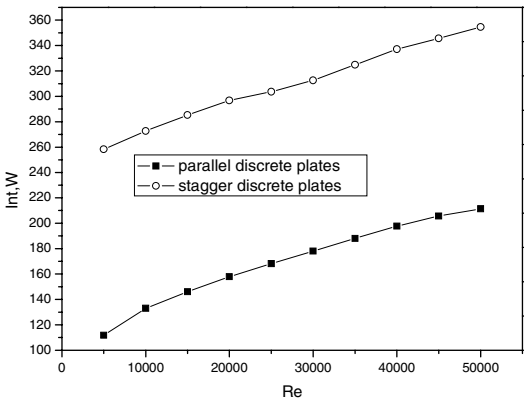

(a) Variation of Int with Reynolds number

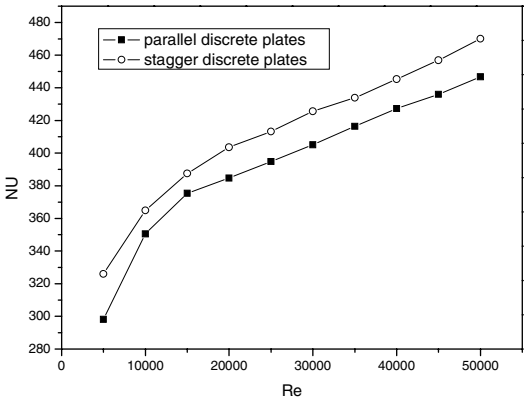

(b) Variation of *Nu* with Reynolds number

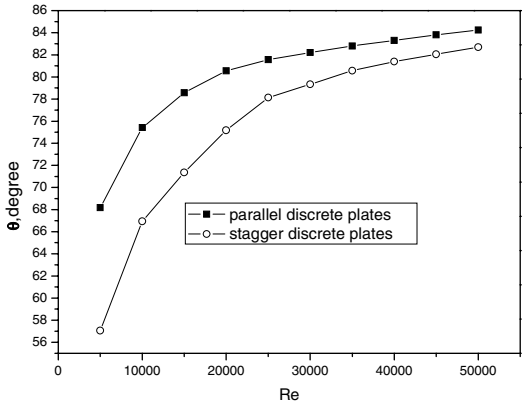

(c) Variation of θ with Reynolds number

FIGURE 8. Results for $d = 2$ mm.

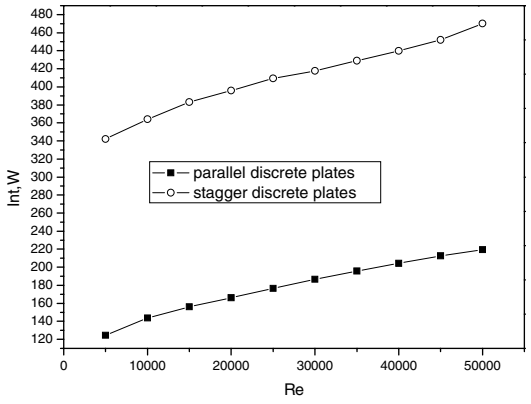

(a) Variation of Int with Reynolds number

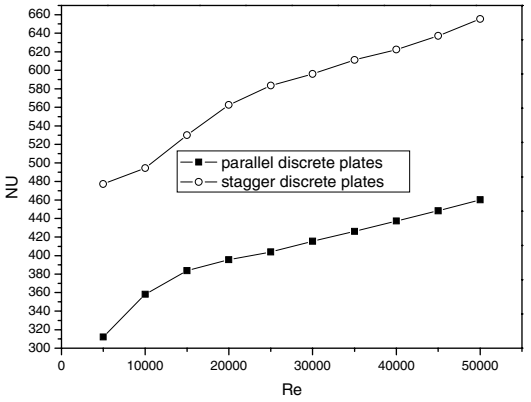

(b)Variation of Nu with Reynolds number

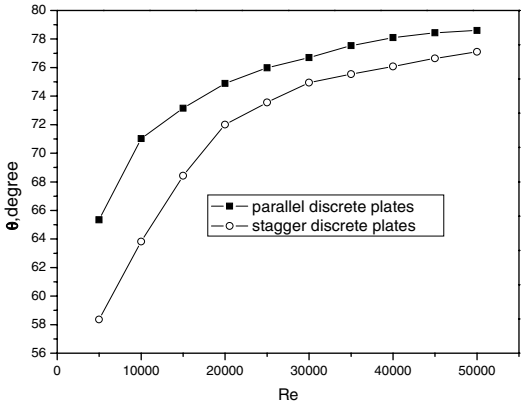

(c) Variation of θ with Reynolds number

FIGURE 9. Results for $d = 4$ mm.

COMPARISON BETWEEN DISCRETE PARALLEL PLATES AND DISCRETE STAGGERED PLATES

It is well known that discrete staggered plates have a better heat transfer performance than discrete parallel plates at the same conditions. Here we compared the values of *Int*, *Nu,* and θ between these two configurations for d = 2 and 4 mm. The Reynolds number is from 5,000 to 50,000. The numerical results are shown in Figures 8 and 9, respectively. We can see that both *Int* and *Nu* of the staggered plates are much higher than those of the parallel plates. However, the intersection angle θ of the discrete staggered plates is smaller than those of the discrete parallel plates. Figures 8 and 9 once again indicate that the field synergy principle is applicable to the turbulent flow and heat transfer.

CONCLUSION

In this paper, the field synergy principle is briefly reviewed. According to this principle, reducing the intersection angle between the velocity and the temperature gradient can enhance the convective heat transfer. Two numerical examples are provided to show the validity of the principle for the turbulent flow and heat transfer situations.

ACKNOWLEDGMENTS

This work was supported by the National Key Project for R&D of China (G2000026303).

REFERENCES

Guo, Z.Y., Li, D.Y., and Wang, B.X. (1998) A Novel Concept for Convective Heat Transfer Enhancement, *Int. J. Heat Mass Transfer*, Vol. 41, pp. 2221–2225.

Jones, W.P. and Lauder, B.E. (1973) The Calculation of Low-Reynolds-Number Phenomena with a Two-Equation Model of Turbulence, *Int. J. Heat Mass Transfer*, Vol. 16, pp. 1119–1130.

Tao, W.Q., Guo, Z.Y., and Wang, B.X. (2002) Field Synergy Principle for Enhancing Convective Heat Transfer—its Extension and Numerical Verifications, *Int. J. Heat Mass Transfer*, Vol. 45, pp. 3849–3856.

Tao, W.Q., He, Y.L., Wang Q.W., Qu Z.G., and Song F.Q. (2002) A Unified Analysis on Enhancing Single Phase Convective Heat Transfer with Field Synergy Principle. *Int. J. Heat Mass Transfer,* Vol. 45, pp. 4871–4879.

Tao, W.Q. (2001) *Numerical Heat Transfer, Second edition*, Xi'an: Xi'an Jiaotong University Press, pp. 350–351.

Tao, W.Q. (2000) *Recent Advances in Computational Heat Transfer,* Beijing: Science Press, pp. 159–162.

Van Doormaal J.P. and Raithby, G.D. (1984) Enhancement of the SIMPLE Method for Predicting Incompressible Fluid Flows, *Numerical Heat Transfer*, Vol. 106, pp. 789–796.

Wang, S., Li, Z.X. and Guo, Z.Y. (1998) Novel Concept and Device of Heat Transfer Augmentation, in: *Proceedings of 11th IHTC* Vol. 5, pp. 405–408.